Catalysis Science & Technology

PAPER

View Article Online
View Journal | View Issue

Cite this: *Catal. Sci. Technol.*, 2015, 5, 4108

Re-evaluating selectivity as a determining factor in peroxidative methane oxidation by multimetallic copper complexes†

David Palomas,[a] Christos Kalamaras,[b] Peter Haycock,[a] Andrew J. P. White,[a] Klaus Hellgardt,[b] Andrew Horton[c] and Mark R. Crimmin*[a]

Received 27th March 2015,
Accepted 17th June 2015

DOI: 10.1039/c5cy00462d

www.rsc.org/catalysis

A series of multimetallic copper(II) complexes have been re-investigated for methane oxidation with H_2O_2. The preparation and properties of trinuclear copper(II) complexes of the form $[Cu_3(triazole)_n(OH_2)_{12-n}]$ (n = 8, 10) are reported. While these complexes are trimeric in the solid-state, ^{1}H NMR studies suggest that facile ligand dissociation occurs in solution. The oxidation of cyclohexane with H_2O_2 catalyzed by $[Cu_3(triazole)_n(OH_2)_{12-n}]$ (n = 8, 10) is compared against a literature known oxo-centered tetrameric cluster (*Angew. Chem., Int. Ed.*, 2005, **44**, 4345) and these catalysts display moderate activities. The series have also been investigated in methane oxidation at 30 bar and 40 °C. Analytical techniques including a solvent suppression ^{1}H NMR method have been applied to quantify the liquid- and gas-phase products. The multimetallic copper(II) complexes and copper(II) nitrate control samples produce only methanol and CO_2. While TONs for methanol production range from 1.4–4.6 in all cases approximately 50 times the amount of CO_2 is produced relative to methanol. We conclude that selectivity is a determining factor in methane oxidation under these conditions and should be considered in future studies.

1. Introduction

The structural correlation between the postulated active site of particulate methane mono-oxygenase (pMMO) and methane oxidizing zeolite Cu-ZSM-5 has provoked interest in the use of multi-metallic copper complexes for methane oxidation.[1] In 2010, Rosenzweig and co-workers cloned and expressed in *E. coli*. a series of water-soluble proteins that correspond to small fragments of the enzyme pMMO. One conclusion of this study was that the most likely active site of the enzyme is comprised of a dicopper cofactor ligated by a series of histidine residues.[2] Schoonheydt and co-workers have concluded that methane oxidation can occur at a similarly dinuclear, bent bis(μ-oxo)dicopper core stabilized on ZSM-5 or mordenite zeolites.[3] Furthermore, the direct oxidation of methane with O_2 can be catalyzed by copper ions on mesoporous silica SBA-15, with the selective formation of formaldehyde.[4]

While these studies have prompted renewed investigation of dinucleating ligand systems capable of the stabilisation of dicopper complexes and the study of their oxidation chemistry,[5] catalytic studies of methane oxidation are limited.[6–8] For example, in 2005 Pombeiro and co-workers reported a series of tri- and tetrametallic copper(II) complexes supported by ethanolamine ligands capable of not only the peroxidative oxidation of cyclohexane but also methane.[6] In late 2010, a patent was filed describing the use of a series of triazole ligands to support putative bimetallic copper(II) complexes capable of methane oxidation with some exceptional activities and liquid-phase selectivities.[7] More recently, inspired by the hypothesis that pMMO oxidises methane at a trimetallic rather than bimetallic site, Chan and co-workers disclosed a series of trinucleating ligands believed to stabilise a tricopper complex capable of the peroxidative oxidation of methane to methanol with turnover numbers (TON) of up to 18 for reactions conducted in H_2O at atmospheric pressure and ambient temperature (Fig. 1).[8] While the authors suggest a model based upon a hydrophobic effect to explain the stability of methanol to over-oxidation, no analysis is presented on the potential gaseous products of over-oxidation, CO and CO_2.[8b]

Herein we re-investigate Pombeiro's ethanolamine-based catalyst[6] and describe the preparation and properties of a series of triazole-based catalysts which, while previously claimed as potent methane oxidation catalysts, are ill-described in terms of synthesis, structure and catalytic

[a] *Department of Chemistry, Imperial College London, South Kensington, London, SW7 2AZ, UK. E-mail: m.crimmin@imperial.ac.uk*
[b] *Department of Chemical Engineering, Imperial College London, South Kensington, London, SW7 2AZ, UK*
[c] *PTI/RE Experimentation, Emerging Technologies Shell Global Solutions International B.V, P.O Box 38000, 1030 BN, Amsterdam, The Netherlands*

† Electronic supplementary information (ESI) available. CCDC 1028073–1028074. For ESI and crystallographic data in CIF or other electronic format see DOI: 10.1039/c5cy00462d

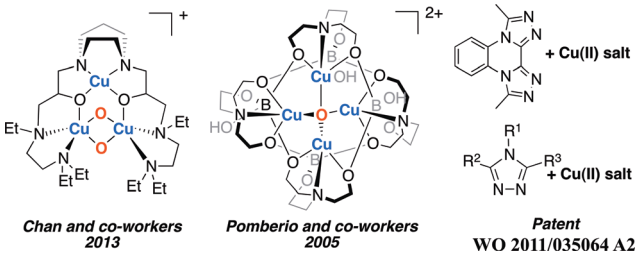

Fig. 1 Multi-metallic Cu-based methane oxidation catalysts.

procedure.[7] We report analytical methods to elucidate both the liquid- and gas-phase products formed from peroxidative oxidation of methane. We conclude that selectivity is *a determining factor* in these reactions and that reporting mass balance for the carbon containing products is an essential approach to properly evaluating catalyst performance.

2. Experimental section

For the preparation of the triazole ligands including a bis(triazole) and the details of the cyclohexane oxidation studies see the ESI.†

General procedure for the synthesis of 3a–d

A solution of $[Cu(NO_3)_2{\cdot}2.5H_2O]$ in acetonitrile was added to a solution of an equimolar amount of triazole ligand in acetonitrile. The reaction mixture was stirred for 3 days at 30 °C, a blue precipitate was observed. The product was isolated by filtration, washed with acetonitrile and hexane and dried under vacuum for 24 h at 25 °C.

3a: a solution of **2a** (1 mmol, 145 mg) in MeCN (4 mL) and was added to $Cu(NO_3)_2{\cdot}2.5H_2O$ (1 mmol, 232 mg) in MeCN (4 mL). After 3 days stirring at 30 °C **3a** was isolated as a blue solid (153 mg, 0.074 mmol, 75%). Infrared (ATR cell, cm^{-1}) 3120, 1598, 1551, 1440, 1286, 1073, 776. UV-vis (H_2O, 25 °C) 221 (ε = 74 600 $dm^3\ mol^{-1}\ cm^{-1}$), 279 (sh, ε = 8790 $dm^3\ mol^{-1}\ cm^{-1}$). Mass spec. (ESI, +ve mode) 493.9 [30%, $Cu_2(\mathbf{2a})_2(dmso)$], 415.0 [100%, $Cu_2(\mathbf{2a})_2$] 353.6 [30%, $Cu(\mathbf{2a})_2$]. Repeated attempts to acquire satisfactory CHN analysis failed.

3b: a solution of **2b** (2.4 mmol, 352 mg) in MeCN (12 mL) was added to $Cu(NO_3)_2{\cdot}2.5H_2O$ (2.4 mmol, 557 mg) in MeCN (8 mL). After 3 days stirring at 30 °C, **3b** was isolated as a blue solid (460 mg, 0.26 mmol, 87% yield). Infrared (ATR cell, cm^{-1}) 3121, 1557, 1448, 1390, 1289, 1023, 757. UV-vis (H_2O, 25 °C) 228 (ε = 22 000 $dm^3\ mol^{-1}\ cm^{-1}$). 265 nm (ε = 14 500 $dm^3\ mol^{-1}\ cm^{-1}$). Mass spec. (ESI, +ve mode) 390.9 (30%, $Cu(\mathbf{2b})_2(OH_2)_2$), 280.9 [100%, $Cu(\mathbf{2b})(OH_2)_4$], 263.9 [75%, $Cu(\mathbf{2b})(OH_2)_3$], 243.9 [40%, $Cu(\mathbf{2b})(OH_2)_2$], 227.0 [60%, $Cu(\mathbf{2a})(OH_2)$]. Elemental analysis calc. for $C_{56}H_{57}Cu_3N_{38}O_{22.5}$: C, 37.10; H, 3.17; N, 29.36 found C, 37.14; H, 3.25; N, 29.34.

3c: a solution of $Cu(NO_3)_2{\cdot}2.5H_2O$ (208 mg, 0.9 mmol) in MeCN (5 mL) was added to a solution of **2c** (143 mg, 0.9 mmol) in MeCN (5 mL). Precipitation of a blue solid is observed immediately and the reaction mixture was stirred for 3 days at 30 °C. **3c** was as a light blue powder (170 mg, 0.252 mmol, 28%). Mass spec. (ESI, +ve mode) 263.9 [75%, $Cu(\mathbf{2c})(NCMe)$], 419.0 [40%, $Cu(\mathbf{2c})_2(OH_2)_2$], 497.0 [20%, $Cu(\mathbf{2c})_2(dmso)(OH_2)_2$]. UV-vis ($H_2O$, 25 °C) 204 (sh, ε = 27 900 $dm^3\ mol^{-1}\ cm^{-1}$), 261 (ε = 2010 $dm^3\ mol^{-1}\ cm^{-1}$). Infrared (ATR cell, cm^{-1}) 3131, 1561, 1459, 1287, 1018, 707. Elemental analysis calc. for $C_{18}H_{18}Cu_2N_{10}O_{12}$ C, 31.18; H, 2.62; N, 20.20 found C, 31.32; H, 2.58; N, 20.05.

3d: a solution of $Cu(NO_3)_2{\cdot}2.5H_2O$ (105 mg, 0.45 mmol) in MeCN (3 mL) was added to a solution of **2d** (73 mg, 0.45 mmol) in MeCN (3 mL). Precipitation of a blue solid is observed immediately and the reaction mixture was stirred for 3 days at 30 °C. The product was as a light blue powder (85 mg, 0.126 mmol, 27%). UV-vis (H_2O, 25 °C) 219 nm (ε = 16 220 $dm^3\ mol^{-1}\ cm^{-1}$), 266 nm (ε = 7150 $dm^3\ mol^{-1}\ cm^{-1}$). Mass spec. (ESI, +ve mode) 381.09 [100%, $Cu(\mathbf{2d})_2$]. Infrared (ATR cell, cm^{-1}) 3126, 1598, 1551, 1439, 1354, 1299, 1074, 782. Elemental analysis calc. for $C_{16}H_{16}Cu_2N_{12}O_{12}$ C, 27.63; H, 2.32; N, 24.17 found C, 27.51; H, 2.41; N, 23.98.

Single-crystal X-ray diffraction data

Although single crystal X-ray diffraction studies of **3b** (ref. 9) and **4** (ref. 6) have been conducted previously, in both cases the compounds crystallised as polymorphs of the known structures. While analysis of single crystals of complex **3a** confirmed the connectivity represented in Scheme 1, these data were not of publishable quality. Data are provided in Fig. 3 and 5 and Table 1, these are included to demonstrate catalyst characterisation.

Methane oxidation

Experiments were carried out in a reactor containing a Teflon-lined vessel with a total volume of 50 mL. The vessel was charged with the catalyst (0.017 mmol), 15 mL solvent, an aqueous solution of H_2O_2 (30 wt%, 5 mL, 50 mmol) and HNO_3 (70 wt% in H_2O, 65 μL, 1 mmol). After sealing, the reactor was purged with methane (4×, P = 30 bar) and then pressurised to 30 bar. The reactor was heated to the desired temperature and vigorously stirred with a Teflon coated magnetic bar at 1500–2000 rpm. After the reaction time is finished the reactor was cooled with an ice-water bath, degassed

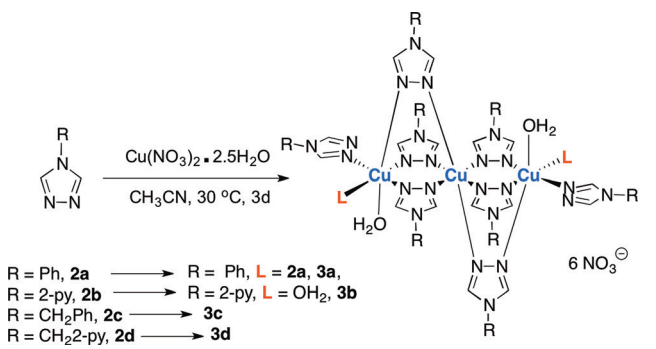

Scheme 1 Preparation of Cu-triazole complexes.

Table 1 Selected acquisition data from single-crystal diffraction experiments

Data	3b	4
Molecular formula	$C_{56}H_{56}Cu_3N_{32}O_4{\cdot}6(NO_3){\cdot}0.5(H_2O)$	$C_{24}H_{52}B_4Cu_4N_4O_{17}[BF_4]_2$
Formula weight (g mol^{-1})	1813.01	1139.71
Crystal system	Triclinic	Monoclinic
Space group	$P\bar{1}$	$C2/c$
Temperature (K)	173	173
a (Å)	14.1016(5)	14.4651(5)
b (Å)	14.4022(6)	19.3815(6)
c (Å)	20.4554(9)	14.1054(5)
α (deg)	94.939(4)°	—
β (deg)	95.386(3)°	90.991(3)
γ (deg)	119.157(4)°	—
V (Å^3)	3570.2(3)	3953.9(2)
Z	2	4
μ (mm^{-1})	0.991	2.237
ρ (g cm^{-3})	1.687	1.915
R_1 (obs)[a]	0.0401	0.0341
wR_2[a] (all data)	0.1021	0.0846
Unique/observed reflections	13 924/10 946	4161/3590
R_{int}	0.0191	0.0261

[a] $R_1 = \sum||F_o| - |F_c||/\sum|F_o|$; $wR_2 = \{\sum[w(F_o^2 - F_c^2)^2]/\sum[w(F_o^2)^2]\}^{1/2}$; $w^{-1} = \sigma^2(F_o^2) + (aP)^2 + bP$.

and opened. Samples were filtered before being analyzed by GC-FID and ^{1}H NMR spectroscopy. Liquid phase analytes were quantified by comparison to standard samples of known concentration.

Analytical methods

Liquid-phase products of methane oxidation were analyzed by GC-FID using an Agilent 7820 equipped with a DB-WAX column and a double solvent suppression ^{1}H NMR method. ^{1}H NMR spectra were measured at a frequency of 500.13 MHz using a Bruker AVANCE III HD 500 spectrometer operating at 298 K. A small amount of D_2O was added to the sample. Double solvent suppression (HOD/CH_3CN), along with ^{13}C decoupling to remove ^{13}C satellite signals was achieved using the pulse program wetdc. All relevant parameters were selected automatically *via* execution of the Bruker AU program au_lc1d after obtaining a ^{1}H NMR spectrum showing the solvent chemical shifts.

The custom-made apparatus shown in Fig. 2 allowed quantification of the gas-phase products from the selective oxidation of methane over homogeneous copper catalysts. The autoclave reactor was charged as described above. After 20 h, the loop (0.5 mL) was filled by the product gas from the exit of the reactor and injected by a 6-way chromatographic valve with electrical actuator to the mass spectrometer (European Spectrometry System II) for analysis using a constant flow of carrier gas (Ar, 300 mL min^{-1}). The mass numbers (m/z), 15 (CH_3^+), 16 (CH_4), 18 (H_2O), 28 (CO), 31 (CH_3O^+), 32 (O_2) and 44 (CO_2) were continuously monitored using Quadstar 32bit software. The purity of the gases used (*e.g.*, CH_4, CO_2, Ar) all provided by BOC gases UK was higher than 99.95%. The amount of CO_2 (μmol) is calculated based on multiplying the area under the CO_2 molar fraction peak (ppm s) with the carrier gas molar flow rate (mol s^{-1}).

3. Results and discussion

Catalyst preparation

Condensation of amines and *N*,*N*-dimethylformamide azine dihydrochloride (**1**) allowed preparation of a series of 4-substituted triazoles (R = Ph, **2a**; 2-Py, **2b**; Bn, **2c**; $CH_2$2-Py, **2d**).[10] Triazole-based copper complexes of ligands **2a–d** were generated from a 1 : 1 reaction between the triazole and Cu(II) salt at 30 °C. Complexes **3a–d** were obtained from [$Cu(NO_3)_2{\cdot}2.5H_2O$] in CH_3CN (Scheme 1).[9] In all cases, complexes precipitated from the reaction media and were isolated as blue solids by filtration. The copper(II) complexes have been characterized by a combination of ^{1}H NMR, UV-vis and infrared spectroscopy, CHN analysis, mass spectrometry and single-crystal X-ray diffraction studies.

X-ray diffraction experiments on single crystals of **3a** and **3b** grown from slow evaporation of concentrated aqueous solutions revealed a structural motif that has been observed

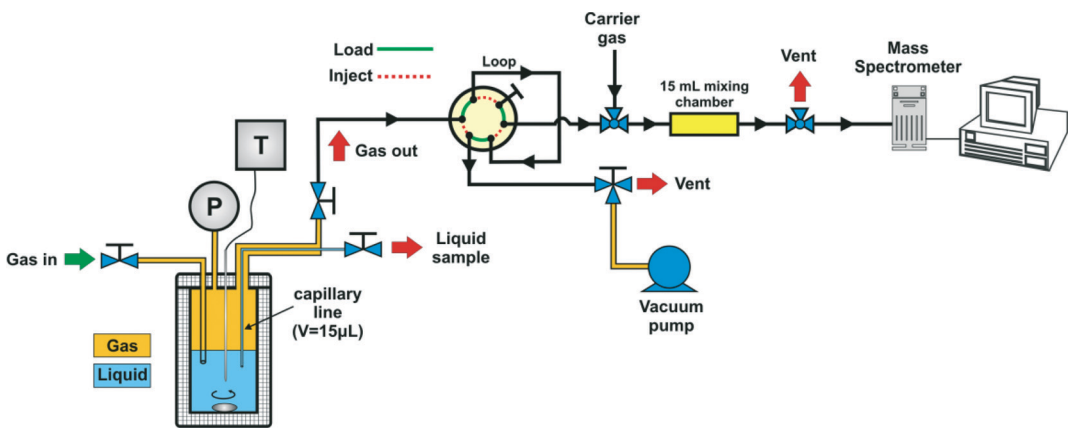

Fig. 2 Apparatus for analysis and quantification of gas-phase analytes.

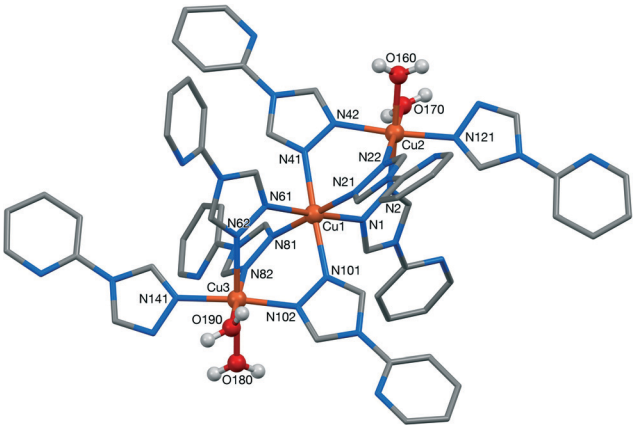

Fig. 3 The crystal structure of **3b**. H-atoms omitted for clarity. Selected bond lengths (Å), Cu(1)–N(21) 1.996(2), Cu(1)–N(81) 2.023(2), Cu(1)–N(101) 2.170(2), Cu(1)–N(1) 2.205(2), Cu(1)–N(41) 2.218(2), Cu(2)–N(42) 2.002(2), Cu(2)–O(160) 2.039(2), Cu(2)–O(170) 2.321(2).

previously.[9] Hence, in the solid state both **3a** and **3b** exist as a tricopper array in which an octahedral central copper atom is complexed by the nitrogen of six triazole ligands (Fig. 3). These ligands bridge to two terminal copper atoms through coordination of the α-heteroatom and the coordination sphere at each terminus is completed by either an additional triazole ligand or H_2O. While both complexes can be related by an S_2-symmetry operation in the solid-state, **3a** takes the form $[Cu_3(\mathbf{2a})_{10}(OH_2)_2]$ and **3b** $[Cu_3(\mathbf{2b})_8(OH_2)_4]$ and these two species differ due to the number of water/triazole ligands coordinated to the terminal copper atoms (Scheme 1). Attempts to grow single crystals of **3c** and **3d** failed.[11]

UV-vis measurements on aqueous solutions of **3a–d** display a maxima at very short-wavelengths with an associated shoulder shifted to slightly longer wavelengths and tailing into the visible region (Fig. 4). These absorptions are tentatively assigned to a π → π* of the triazole ligand and MLCT respectively. For example, **3a** demonstrates transitions at 221 and 279 nm. Complexes **3b** and **3d** also show a second maxima centred close to 270 nm overlapping the shoulder and

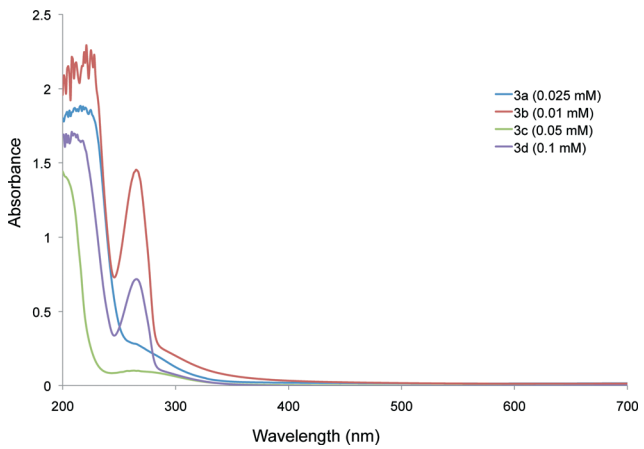

Fig. 4 UV-vis data on **3a–d**.

assigned to the n → π* transition of the pyridine unit within these complexes.[12] Mass spectrometry on samples **3a–d** revealed a series of peaks with *m*/*z* consistent with mono- and dicopper fragments. Using electrospray ionization, peaks associated with the intact trimeric structures of **3a** or **3b** were not observed. In the infrared spectra, the C=N stretches of the triazole moiety of **3a–d** are observed between 1551–1598 cm^{-1} and differ only slightly from those of the free ligand. Magnetic measurements have been made on **3b** previously.[12]

Despite their paramagnetic nature, ^{1}H NMR data collected on **3a** and **3b** in D_2O demonstrate the expected resonances albeit broadened and within the chemical shift window δ = 5–25 ppm. In solution, only one ligand environment is observed by ^{1}H NMR spectroscopy. Analysis of the X-ray data suggests that at least three environments should be present in the static structure (one terminal and two bridging, *trans*- and *cis*- to the unique terminal ligand). Upon mixing of samples of **3a** and **3b** in D_2O only two ligand environments are observed by ^{1}H NMR spectroscopy one for triazole **2a** and a second for triazole **2b**. Furthermore, addition of samples of **2a** to trimeric copper complex **3b** in either D_2O or dmso-d_6 gives data consistent with a mixture of **3a** and **3b** in solution. In order to obtain an idea of the aggregation state of the species observed in solution by ^{1}H NMR spectroscopy we performed a series of DOSY experiments. Diffusion coefficients were measured at 25 °C in d_6-dmso for **2a–d** (0.1–0.2 M, D = 3.9–4.2 × 10^{-10} m^2 s^{-1}) and **3a–b** (0.01 M, D = 2.6–3.1 × 10^{-10} m^2 s^{-1}).[13]

The DOSY data suggest that the triazole ligand environments observed by ^{1}H NMR spectroscopy are not associated with a large trimetallic cluster. In combination with the cross-over experiments these data can be accounted for by two processes: (i) the reversible dissociation of the terminal ligand of the trimeric complexes **3a–b** in solution and the observation of the time-averaged ^{1}H NMR environment of the triazole contact shifted by the paramagnetic copper complex or (ii) disintegration of the cluster to monomeric species including $[Cu(triazole)_n(OH_2)_{6-n}]$ (n = 3, 4) in solution and facile inter- and intra-molecular ligand exchange within the isomers of this series. A monomeric octahedral Mn complex of ligand **2b** has been reported previously.[14]

The oxo-centered tetrameric copper cluster **4** was obtained as green crystals according to the procedure reported by Pombeiro and co-workers.[6] Analysis of **4** from a series of preparations provided suitable mass spectrometry and single crystal data on **4** that is consistent with the literature (Fig. 5).

Cyclohexane oxidation

As a means to benchmark the catalysts we investigated the oxidation of cyclohexane. Reactions were conducted in MeCN using aq. H_2O_2 as an oxidant and HNO_3 as an additive. Complex **4** was originally reported by Pombeiro and co-workers for cyclohexane oxidation at 25 °C and data were reproduced with independently synthesized samples with minor modification of the catalyst/peroxide ratio (Table 2, entries 1 and 2).[6]

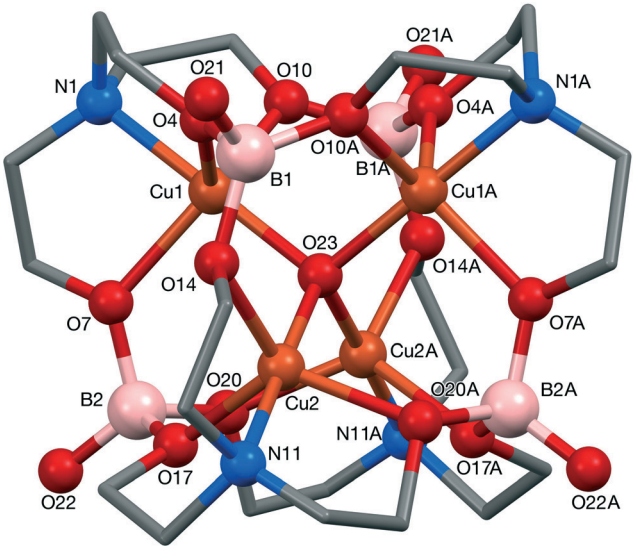

Fig. 5 The crystal structure of **4**. H-atoms omitted for clarity, selected bond lengths (Å), Cu(1)–O(23) 1.9253(15), Cu(1)–N(1) 2.000(2), Cu(1)–O(4) 2.029(4) Cu(1)–O(10) 2.031(4), B(1)–O(4) 1.510(5), B(1)–O(4′) 1.437(6).

Under similar conditions **3a–d** give similar turnover numbers (10.3–17.5) and selectivity with a bias towards forming the alcohol (cyclohexanol, 68–77%; cyclohexanone, 23–32%). Reducing the catalyst concentration by a factor of 10 resulted in a 5000 : 1 ratio of peroxide to catalyst and improved catalyst activity. Pombeiro and co-workers first suggested using low catalyst loadings and high peroxide to catalyst ratios to improve catalyst performance.[17] Under these conditions **3a–d** oxidized cyclohexane with higher turnover numbers (80.6–90.6) and lower selectivities (cyclohexanol, 60–62%; cyclohexanone, 40–38%). Control experiments with $[Cu(NO_3)_2 \cdot 2.5H_2O]$ under the optimized conditions gave only trace amounts of oxidation products. Furthermore attempts to generate active catalysts *in situ* by mixing $[Cu(NO_3)_2 \cdot 2.5H_2O]$ with **2a** or **2b** did not reproduce the activity of as isolated samples of **3a** or **3b** respectively.

The catalytic activities are approximately an order of magnitude lower than those reported in the patent literature,[7] but are comparable to a series of recently reported multimetallic copper complexes. For example, Roy and co-workers have reported a series of tetranuclear Cu(II) Schiff-base complexes for the oxidation of cyclohexane with TONs of approximately 10–20 and a slight selectivity for cyclohexanol.[15] While Chan, Yu and coworkers have reported a series of trinuclear copper complexes with activities commensurate with those of **3a–b**,[8b,16] Pombeiro, Shul'pin and co-workers have reported a significant number copper(II) multi-metallic clusters based on chelating N,O-based ligands with a range of activities some of which exceed the optimized activity of **3a–b**.[18] A number of studies have demonstrated the positive effect of small amounts of acid in peroxidative alkane oxidation and control experiments conducted without HNO_3 resulted in lower catalyst activities. While the beneficial effect of the acid is not entirely clear, one possibility is that the acid helps to slow the decomposition of the peroxide.[17,19]

Methane oxidation

The oxidation of methane was performed with catalysts **3a–b** and **4** in liquid–gas phase experiments using 1000–3000 equiv. of H_2O_2 per equiv. of catalyst. Reactions were conducted at 3 bar MeH at 40 °C using a Teflon lined batch reactor. While previous studies have reported **4** and triazole-based catalysts for methane oxidation, full analysis of the both the liquid and gas-phase analytes has not been forthcoming.[6,7] As such, the selectivities of these reactions are unknown and the usefulness of the catalyst cannot be accurately evaluated.

A series of analytical methods were developed to address this problem. Liquid-phase oxidation products were analyzed by a combination of GC-FID analysis and a double-solvent suppression ^{1}H NMR method.[20] Based on the work of Hutchings and co-workers,[21] an ^{1}H NMR method was developed that allows quantitative analysis of C_1- and C_2-oxidation products MeOH, EtOH, HCO_2H, MeC(O)H in mixtures of proteo-water and acetonitrile (Fig. 6). Both formaldehyde and acetic acid are not observed in this experiment and while we attribute this to reversible exchange of $H_2C(OH_2)_2$ with H_2O and overlap of the diagnostic methyl resonance of $MeCO_2H$ with that of the suppressed MeCN signal, acetic acid is readily quantified by GC-FID. Quantitative gas-phase analysis of CO_2 was performed by sampling of an aliquot directly from the high-pressure reactor, diluting with a known volume of a carrier gas and analyzing by mass spectrometry. While this method also has the capacity to quantify CO and O_2/MeH, the former was not observed during methane oxidation and the latter do not provide direct information about the selectivity of methane oxidation.

Complexes **3a–b** and **4** proved active for the oxidation of methane to methanol (Table 3, entries 1–3). In all cases both the liquid- and gas-phase analytes were quantified. Comparison of the data in Table 3 reveals that the double solvent-suppression NMR method reproduces the GC-FID data for the quantification of methanol within acceptable error. While in all cases, triazole based catalysts **3a–b** demonstrated a higher activity for methanol production than **4**, TONs for MeOH for the series range from 1.4–4.6. These data are consistent with a recent report of Chan and coworkers that demonstrated a trimeric copper catalyst capable of methane oxidation to methanol with a TON of up to 18 using portionwise addition of 100 equiv. of H_2O_2.[8] These studies have demonstrated that the productive catalytic cycle is competitive with an abortive cycle that consumes further equivalents of H_2O_2 and that optimal TONs can be achieved by controlled addition of the H_2O_2 to the reaction mixture. Based on data from lower TON experiments (TON = 6), using 20 equiv. of H_2O_2 Chan and coworkers suggest an efficient and selective reaction which produces approximately 1 equiv. of methanol per 3 equiv.

Table 2 Cyclohexane oxidation with isolated multi-metallic copper(II) complexes

Entry	Catalyst	Ratio of H_2O_2 : catalyst	t (h)	TON[d] Cyclohexanol	Cyclohexanone	Total[e]
1[a]	**4**/HNO_3	400	72	10.5	4.9	15.3
2[b]	**4**/HNO_3	500	72	11.4	3.8	15.2
3[b]	**3a**/HNO_3	500	20	12.7	4.2	16.9
4[b]	**3b**/HNO_3	500	20	13.5	4.0	17.5
5[b]	**3c**/HNO_3	500	20	7.1	3.2	10.3
6[b]	**3d**/HNO_3	500	20	7.5	3.5	11.0
7[c]	**3a**/HNO_3	5000	20	49.8	30.8	80.6
8[c]	**3b**/HNO_3	5000	20	54.1	36.5	90.6
9[c]	$Cu(NO_3)_2$/HNO_3	5000	20	0	0	0

[a] Data from ref. 6. Catalyst (0.0125 mmol), H_2O_2 (5 mmol), cyclohexane (0.63 mmol), HNO_3 (0.12 mmol), 25 °C. [b] Catalyst (0.01 mmol), H_2O_2 (5 mmol), cyclohexane (5 mmol), HNO_3 (0.2 mmol). [c] Catalyst (0.001 mmol), HNO_3 (0.02 mmol). [d] Turnover number (moles of product per mol of catalyst) analysed by GC-FID using chlorobenzene as internal standard. [e] Cyclohexanol + cyclohexanone.

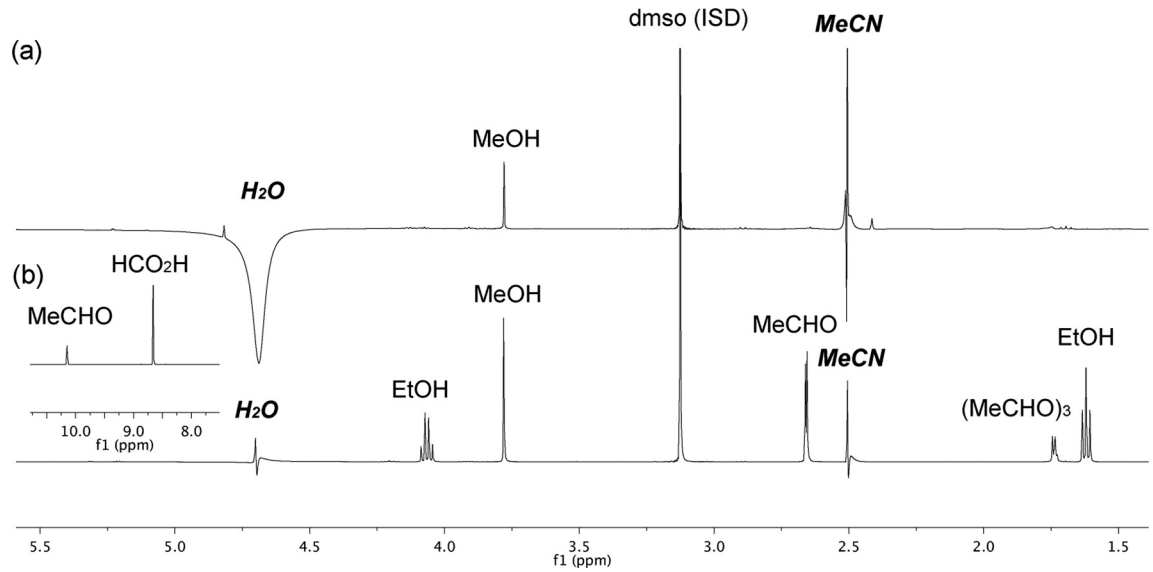

Fig. 6 (a) Liquid phase analytes from the oxidation of methane catalysed by **4**. (b) Double solvent-suppression NMR method for the quantification of liquid-phase analytes of methane oxidation, inset is the downfield region showing the deshielded resonances of MeCHO and HCO_2H.

Table 3 Methane oxidation with isolated multi-metallic copper(II) complexes **3a–b**, **4** and $[Cu(NO_3)_2{\cdot}2.5H_2O]$

Entry	Catalyst	Ratio of H_2O_2 : catalyst	HCO_2H (μmol)	EtOH (μmol)	$MeCO_2H$ (μmol)	MeCOH (μmol)	CO (μmol)	CO_2 (μmol)	MeOH GC[c] (μmol)	MeOH NMR[d] (μmol)	TON[e]
1[a]	**3a**/HNO_3	3000	0	0	0	0	0	3700	64.0	57.1	3.4–3.8
2[a]	**3b**/HNO_3	3000	0	0	0	0	0	3900	73.5	77.9	4.3–4.6
3[b]	**4**/HNO_3	1000	0	0	0	0	0	3650	69.4	71.6	1.4
4[a]	$Cu(NO_3)_2$/HNO_3	3000	0	0	0	0	0	3000	43.8	34.9	2.1–2.6

[a] Reaction conditions: catalyst (0.017 mmol), H_2O_2 (50 mmol), HNO_3 (1 mmol), methane (30 bar), V = 20 mL. [b] The literature conditions ref. 6 were scaled to V = 20 mL, catalyst (0.05 mmol), H_2O_2 (50 mmol), HNO_3 (1 mmol), methane (30 bar). [c] Analysed by GC-FID. [d] Analysed by ^{1}H-NMR following a solvent suppression protocol, DMSO as internal standard. [e] Turnover number (moles of product per mol of catalyst).

of H_2O_2. No analysis of the gas phase products has been forthcoming.

In the current case, analysis of the gas-phase analytes reveals production of significant quantities of CO_2. For example, the reaction of methane with **4**, 1000 equiv. of H_2O_2 and a HNO_3 : catalyst ratio of 20 produces 70 ±2 μmol of methanol and 3650 μmol of CO_2. A control experiment using $Cu(NO_3)_2 \cdot 2.5H_2O$ in place of **3a–b** or **4** revealed only minor changes on the product distribution suggesting that, in this instance and in the presence of such a large excess of H_2O_2, the ligand sphere has very limited control on the catalytic pathway (Table 3, entry 4). Any comment on the reaction mechanism, or speculation that these catalysts are playing a role other than generating peroxide radicals *in situ*, is unwarranted based on the current data.

The propensity, and precedent,[22] for MeCN to act as a C1-source prompted us to further investigate the reactivity of the solvent under the reported reaction conditions. The decomposition of MeCN to CO_2 was investigated by a further control reaction conducted without MeH, although small amounts of CO_2 where observed (48 μmol) this experiment does not account for the large amounts of CO_2 produced under catalytic conditions. Consistent with the more facile oxidation of methanol than methane under the reaction conditions, approximately 50 times more CO_2 is produced than MeOH regardless of the nature of the catalyst.

4. Conclusions

We have re-investigated a series of triazole- and aminoethanol-based multimetallic copper(II) catalysts for the oxidation of cyclohexane and methane using H_2O_2. We conclude that, regardless of the minor differences in the TON observed for methanol production, selectivity is an important factor in these reactions. If useful homogeneous catalysts are to be developed that reproduce the activity of enzymatic (pMMO) or heterogeneous (M-ZSM-5) systems then selectivity must be considered as a determining factor in these reactions.

Acknowledgements

We are grateful to the Royal Society for the provision of a University Research Fellowship (MRC). Royal Dutch Shell for project funds (DP, CK).

References

1 (*a*) J. M. Bollinger Jr., *Nature*, 2010, **465**, 40; (*b*) R. A. Himes, K. Barnese and K. D. Karlin, *Angew. Chem., Int. Ed.*, 2010, **49**, 6714; (*c*) R. A. Himes and K. D. Karlin, *Proc. Natl. Acad. Sci. U. S. A.*, 2009, **106**, 18877.

2 (*a*) R. Balasubramanian, S. M. Smith, S. Rawat, L. A. Yatsunyk, T. L. Stemmler and A. C. Rosenzweig, *Nature*, 2010, **465**, 115; (*b*) R. Balasubramanian and A. C. Rosenzweig, *Acc. Chem. Res.*, 2007, **40**, 573.

3 (*a*) M. H. Groothaert, P. J. Smeets, B. F. Sels, P. A. Jacobs and R. A. Schoonheydt, *J. Am. Chem. Soc.*, 2005, **127**, 1394; (*b*) P. J. Smeets, R. G. Hadt, J. S. Woertink, P. Vanelderen, R. A. Schoonheydt, B. F. Sels and E. I. Solomon, *J. Am. Chem. Soc.*, 2010, **132**, 14736.

4 Y. L. An, D. An, Q. Zhang and Y. Wang, *J. Phys. Chem. C*, 2008, **112**, 13700.

5 (*a*) P. Haack and C. Limberg, *Angew. Chem., Int. Ed.*, 2014, **53**, 4282; (*b*) P. Haack, A. Kärgel, C. Greco, J. Dokic, B. Braun, F. F. Pfaff, S. Mebs, K. Ray and C. Limberg, *J. Am. Chem. Soc.*, 2013, **135**, 16148; (*c*) P. Haack, C. Limberg, K. Ray, B. Braun, U. Kuhlmann, P. Hildebrandt and C. Herwig, *Inorg. Chem.*, 2011, **50**, 2133.

6 A. M. Kirillov, M. N. Kopylovich, M. V. Kirillova, M. Haukka, M. F. C. Guedes da Silva and A. J. L. Pombeiro, *Angew. Chem., Int. Ed.*, 2005, **44**, 4345.

7 R. Elgammal and S. Foister, *International Patent*, WO 2011/035064 A2, 2011.

8 (*a*) S. I. Chan, Y.-J. Lu, P. Nagababu, S. Maji, M.-C. Hung, M. M. Lee, I.-J. Hsu, P. D. Minh, J. C.-H. Lai, K. Y. Ng, S. Ramalingam, S. S.-F. Yu and M. K. Chan, *Angew. Chem., Int. Ed.*, 2013, **52**, 3731; (*b*) P. Nagababu, S. S.-F. Yu, S. Maji, R. Ramu and S. I. Chan, *Catal. Sci. Technol.*, 2014, **4**, 930.

9 (*a*) O. G. Shakirova, A. V. Virovets, D. Y. Naumov, Y. G. Shvedenkov, V. N. Elokhina and L. G. Lavrenova, *Inorg. Chem. Commun.*, 2002, **5**, 690; (*b*) J. Liu, Y. Song, Z. Yu, J. Zhuang, X. Huang and X. You, *Polyhedron*, 1999, **18**, 1491.

10 (*a*) A. D. Naik, J. Marchand-Brynaert and Y. Garcia, *Synthesis*, 2008, 149; (*b*) S. B. Muñoz III, W. K. Foster, H.-J. Lin, C. G. Margarit, D. A. Dickie and J. M. Smith, *Inorg. Chem.*, 2012, **51**, 12660.

11 In subsequent experiments a 1 : 1 ligand : metal ratio implied by the CHN analysis is assumed. Possible structural motifs include the coordination of nitrate to Cu. See for example, (*a*) A. F. Stassen, W. L. Driessen, J. G. Haassnoot and J. Reedijk, *Inorg. Chim. Acta*, 2003, **350**, 57; (*b*) S. Amaral, W. E. Jensen, C. P. Landee, M. M. Turnbull and F. M. Woodward, *Polyhedron*, 2001, **20**, 1317.

12 J. A. Joule and K. Mills, *Heterocyclic Chemistry*, 2010, 5th edn., Chichester, Blackwell Publishing.

13 DOSY data were processed within Topspin using the SimFit Alogorithm.

14 B. Ding, L. Yi, P. Cheng, H.-B. Song and H.-G. Wang, *J. Coord. Chem.*, 2004, **57**, 771.

15 P. Roy and M. Manassero, *Dalton Trans.*, 2010, **39**, 1539.

16 (*a*) P. Nagababu, S. Maji, M. P. Kumar, P. P.-Y. Chen, S. S.-F. Yu and S. I. Chan, *Adv. Synth. Catal.*, 2012, **354**, 3275; (*b*) S. I. Chan, C. Y.-C. Chien, C. S.-C. Yu, P. Nagababu, S. Maji and P. P.-Y. Chen, *J. Catal.*, 2012, **293**, 186.

17 T. F. S. Silva, L. M. D. R. S. Martins, M. F. C. Guedes da Silva, M. L. Kuznetsov, A. R. Fernandes, A. Silvam, C.-J. Pan, J.-F. Lee, B.-J. Hwang and A. J. L. Pombeiro, *Chem. – Asian J.*, 2014, **9**, 1132.

18 (*a*) A. M. Kirillov, M. N. Kopylovich, M. V. Kirillova, E. Y. Karabach, M. Haukka, M. F. C. Guedes da Silva and A. J. L. Pombeiro, *Adv. Synth. Catal.*, 2006, **348**, 159; (*b*) C. D. Nicola,

Y. Y. Karabach, A. M. Kirilov, M. Monari, L. Pandolfo, C. Pettinari and A. J. L. Pombeiro, *Inorg. Chem.*, 2007, **46**, 221; (*c*) K. R. Gruenwald, A. M. Kirillov, M. Hauuka, J. Sanchiz and A. J. L. Pombeiro, *Dalton Trans.*, 2009, 2109; (*d*) M. V. Kirillova, A. M. Kirillov, D. Mandelli, W. A. Carvalho, A. J. L. Pombeiro and G. B. Shul'pin, *J. Catal.*, 2010, **272**, 9; (*e*) A. M. Kirillov, M. V. Kirillova, L. S. Shul'pina, P. J. Figiel, K. R. Gruenwald, M. F. C. Guedas da Silva, M. Haukka, A. J. L. Pombeiro and G. B. Shul'pin, *J. Mol. Catal. A: Chem.*, 2011, **350**, 26; (*f*) M. N. Kopylovich, K. T. Mahmudov, M. F. C. Guedes da Silva, P. J. Figiel, Y. Y. Karabach, M. L. Kuznetsov, K. V. Luzyanin and A. J. L. Pombeiro, *Inorg. Chem.*, 2011, **50**, 918; (*g*) R. Jlassi, A. P. C. Ribeiro, M. F. C. Guedes da Silva, K. T. Mahmudov, M. N. Kopylovich, T. B. Anisimova, H. Naïli, G. A. O. Tiago and A. J. L. Pombeiro, *Eur. J. Inorg. Chem.*, 2014, **27**, 4541.

19 R. R. Fernandes, M. V. Kirllova, J. A. L. da Silva, J. J. R. F. da Silca and A. J. L. Pomeiro, *Appl. Catal., A*, 2009, **353**, 107.

20 For WET Solvent Suppression and Its Applications to LC NMR and High-Resolution NMR Spectroscopy see, S. H. Smallcombe, S. L. Patt and P. A. Keifer, *J. Magn. Reson., Ser. A*, 1995, **117**, 295.

21 C. Hammond, M. M. Forde, M. H. A. Rahim, A. Thetford, Q. He, R. L. Jenkns, N. Dimitratos, J. A. Lopez-Sanchez, N. F. Dummer, D. M. Murphy, A. F. Carely, S. H. Taylor, D. J. Willock, E. E. Stangland, J. Kang, H. Hagen, C. J. Kiely and G. J. Hutchings, *Angew. Chem., Int. Ed.*, 2012, **51**, 5129.

22 G. B. Shul'pin, G. V. Nizova, Y. N. Kozlov, L. G. Cuervo and G. Süss-Fink, *Adv. Synth. Catal.*, 2004, **346**, 317.